

The reaction of the pyrophosphate ion with the antitumour complex $\{[\text{CuL}(\text{CH}_3\text{COO})]_2\}$ (HL = 2-formylpyridine thiosemicarbazone) and the single-crystal X-ray structure of $[(\text{CuL})_4\text{P}_2\text{O}_7] \cdot n\text{H}_2\text{O}$

Eric W. Ainscough*, Andrew M. Brodie*, John D. Ranford, Joyce M. Waters*

Department of Chemistry and Biochemistry, Massey University, Palmerston North (New Zealand)

and Keith S. Murray

Department of Chemistry, Monash University, Clayton, Vic. 3168 (Australia)

(Received March 13, 1992)

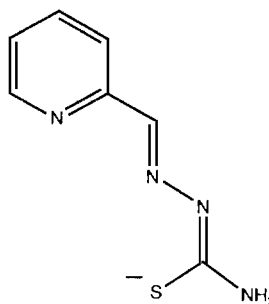
Abstract

The preparation of the complex $[(\text{CuL})_4\text{P}_2\text{O}_7] \cdot n\text{H}_2\text{O}$ (HL = 2-formylpyridine thiosemicarbazone; $n = 9-12$) from the reaction of $\text{Na}_4\text{P}_2\text{O}_7$ with $\{[\text{CuL}(\text{CH}_3\text{COO})]_2\}$ is described. The complex has been characterized by a variety of physicochemical techniques and its crystal and molecular structure determined. Crystals of $[(\text{CuL})_4\text{P}_2\text{O}_7] \cdot n\text{H}_2\text{O}$ are monoclinic, space group $C2/c$, with $a = 29.074(6)$, $b = 28.021(3)$, $c = 13.374(3)$ Å, $\beta = 102.93(2)^\circ$ and $Z = 8$. The complex is tetranuclear, containing four CuL^+ moieties linked by a bridging $\text{P}_2\text{O}_7^{4-}$ anion. Each copper atom is in an approximately square pyramidal environment. The equatorial positions are occupied by a pyrophosphate oxygen, a pyridine nitrogen, an imine nitrogen and a thioamide sulfur, the latter three from the same L ligand. A weakly bound S atom from an adjacent L ligand, is in an axial position, thus completing the coordination sphere. Each tetranuclear $[(\text{CuL})_4\text{P}_2\text{O}_7]$ molecule may be considered as a pair of dinuclear $(\text{CuL}^+)_2$ units linked by a $\text{P}_2\text{O}_7^{4-}$ anion. Each dinuclear unit is further linked by the axial Cu–S bonds. The pyrophosphate ion, which displays a staggered conformation, plays an important role in the hydrogen bonding network involving phosphate oxygens, the thioamide and amine nitrogens of L, and the water molecules in the structure. The variable temperature magnetic susceptibility of $[(\text{CuL})_4\text{P}_2\text{O}_7] \cdot n\text{H}_2\text{O}$ is compared with that of $\{[\text{CuL}(\text{CH}_3\text{COO})]_2\}$ and in both cases the results are interpreted in terms of very weak antiferromagnetic coupling between the copper atoms. In the case of the pyrophosphate complex, the fact that the structure contains dinuclear $(\text{CuL}^+)_2$ units linked in pairs required that an interaction between the dinuclear units as well as the intramolecular J value be included to fit the magnetic data.

Introduction

Although the antitumour complex $\{[\text{CuL}(\text{CH}_3\text{COO})]_2\}$ (HL = 2-formylpyridine thiosemicarbazone) is a dimer in the solid state [1, 2], the active species *in vivo* is undoubtedly the monomeric cation $\text{CuL}^+(\text{aq.})$ [3]. The proposed mechanisms for the drug's antitumour activity, which involve its interaction with nitrogen or sulfur donors [4–7] have been given credence by the isolation of a range of stable 'N' or 'S' Lewis base adducts with the CuL^+ moiety [8]. However, *in vivo* the possibility of oxygen donor adduct formation also exists, whereby the drug binds to the phosphato oxygens of nucleic acids. To model this interaction *in vitro*, we have reacted sodium pyrophosphate, $\text{Na}_4\text{P}_2\text{O}_7$, with the parent dimer, $\{[\text{CuL}(\text{CH}_3\text{COO})]_2\}$, and in this paper report the iso-

lation and characterization of the tetranuclear product, $[(\text{CuL})_4\text{P}_2\text{O}_7] \cdot n\text{H}_2\text{O}$ ($n = 9-12$). As far as we are aware, this is the first X-ray crystallographic study on a ternary pyrophosphato-copper(II) complex.



L

*Authors to whom correspondence should be addressed.

Experimental

Physical measurements were carried out as described previously [8]. The Oxford Instruments Faraday balance used for the magnetic measurements and the linear least-squares fitting methods used to treat the data have been described earlier [9]. The ligand, HL, was synthesized following a published method [10], as was the complex, $[(\text{CuL}(\text{CH}_3\text{COO}))_2]$ [1].

Synthesis of $[(\text{CuL})_4\text{P}_2\text{O}_7] \cdot n\text{H}_2\text{O}$ ($n=9-12$)

To a hot, filtered solution of $[(\text{CuL}(\text{CH}_3\text{COO}))_2]$ (200 mg, 0.33 mmol) in water (70 cm³) was added $\text{Na}_4\text{P}_2\text{O}_7$ (176 mg, 0.66 mmol) in the same solvent (10 cm³). The resulting green solution was filtered and allowed to stand for 2 days, by which time dark green needle-like crystals of the product had formed. These were filtered off and dried by absorbing excess solvent onto filter paper. Yield 45 mg (20%). The number of H₂O molecules of solvation (n) may vary within a sample. Analytical data best fit $n=12$ but the single crystal X-ray analysis indicates at least 13 H₂O sites some of which are only partially occupied. *Anal.* Found: C, 24.7; H, 4.2; N, 16.6; P, 4.9. Calc. for $\text{C}_{28}\text{H}_{58}\text{Cu}_4\text{N}_{16}\text{O}_{19}\text{P}_2\text{S}_4$: C, 24.7; H, 3.9; N, 16.5; P, 4.6%. IR (nujol): 1153, 1085, 933 (νPO) cm⁻¹; Λ (Me₂SO): 4 S cm² mol⁻¹ per Cu. UV-Vis: λ_{max} (nujol) 426, 640(sh) nm; λ_{max} (Me₂SO) 412 (ϵ 11 100), 628 nm (ϵ 110 l mol⁻¹ cm⁻¹). ESR: (powder, at 110 K) g_{\perp} 2.035, g_{\parallel} 2.179; μ_{eff} (at 293 K): 1.83 BM per Cu.

Crystal structure of μ_4 -(pyrophosphato- O, O', O'', O''')-tetrakis[(2-formylpyridine thiosemicarbazonato)-copper(II)]-water (1/ n), $[(\text{CuL})_4\text{P}_2\text{O}_7] \cdot n\text{H}_2\text{O}$

Crystal data

The single crystal of $[(\text{CuL})_4\text{P}_2\text{O}_7] \cdot n\text{H}_2\text{O}$ (HL=2-formylpyridine thiosemicarbazone) selected for data collection displayed faces of the forms {100}, {110}, {010}, {110}, {100}, {110}, {010}, {110}, {001}, {001} and had approximate dimensions of 0.040 × 0.032 × 0.024 cm. It was mounted in air on a CAD4 diffractometer. Cell dimensions, determined from the setting angles of 25 reflections are $a = 29.074(6)$, $b = 28.021(3)$, $c = 13.374(3)$ Å, $\beta = 102.93(2)^\circ$. For a cell volume of 10619.4 Å³ and a molecular weight of 1307.1 amu ($\text{C}_{28}\text{H}_{46}\text{Cu}_4\text{N}_{16}\text{O}_{16}\text{P}_2\text{S}_4$) for $n=9$, the density was calculated to be 1.635 g cm⁻³ for 8 formula weights in the cell. $F(000) = 5248$. Systematic absences (hkl , $h+k=2n+1$; $h0l$, $l=2n+1$) were consistent with the space groups Cc and $C2/c$ (on refinement of the structure $C2/c$ was shown to be correct).

Data collection and processing

A total of 10 503 data was collected with Cu K α radiation ($\mu(\text{Cu K}\alpha) = 44.58 \text{ cm}^{-1}$) using the $\omega/2\theta$ scan technique ($\theta_{\text{max}} = 70^\circ$). A variable scan width of $(1.00 + 0.142 \tan\theta)^\circ$ was calculated for each reflection and this was extended by 25% at both ends of the scan for background measurements. A variable horizontal aperture width of $(1.8 + 0.80 \tan\theta)$ mm was calculated. The vertical aperture was 4 mm. A maximum scan time of 120 s was set for each reflection. The intensities of three standard reflections were monitored during the data collection but the maximum variation was only 2.4%. Absorption corrections were applied, minimum and maximum transmission factors being 0.2364 and 0.6726, respectively.

Structure analysis and refinement

The structure was solved by Patterson and Fourier methods and refined by a blocked full-matrix least-squares technique. The structure contains a number of water molecules distributed over a total of 5 fully and 8 partially occupied sites. The final refinement cycle converged to values of 0.089 and 0.095 for R and R_w , respectively, for the 602 variables and 6087 data for which $F^2 > 5\sigma(F^2)$. The function minimized was $\sum w(|F_o - F_c|)^2$ with the weight w being defined as $2.7994/[\sigma^2(F) + 0.003712F^2]$. Hydrogen atoms were in calculated positions (C-H 0.96 Å) with isotropic thermal parameters assumed. Anisotropic thermal motion was assumed for all non-hydrogen atoms except the water molecules. Atomic scattering factors were taken from the tabulations of Cromer and Mann [11], anomalous dispersion corrections were by Cromer and Liberman [12]. The numbering system is given in Fig. 1, final atomic coordinates for the non-hydrogen atoms are given in Tables 1 and 2. See also 'Supplementary material'.

Results and discussion

The complex $[(\text{CuL})_4\text{P}_2\text{O}_7] \cdot n\text{H}_2\text{O}$, was prepared from the reaction of sodium pyrophosphate with $[(\text{CuL}(\text{CH}_3\text{COO}))_2]$. The IR spectrum shows strong bands at 1153, 1085 and 933 cm⁻¹ confirming the presence of the $\text{P}_2\text{O}_7^{4-}$ anion [13]. The molar conductivity value of 4 S cm⁻¹ mol⁻¹ (in Me₂SO) lies well below the value expected (50–70 S cm⁻¹ mol⁻¹) [14] for 1:1 electrolytes in this solvent, pointing to anion coordination even in solution. Magnetic susceptibility (discussed further below) and ESR data are normal for weakly antiferromagnetically coupled copper(II) centres [15]. The electronic spectrum exhibits a strong band in the 400 nm region which is assigned to a S → Cu(II) ligand-to-metal charge transfer absorption [1, 8, 16] and is typical of complexes containing the

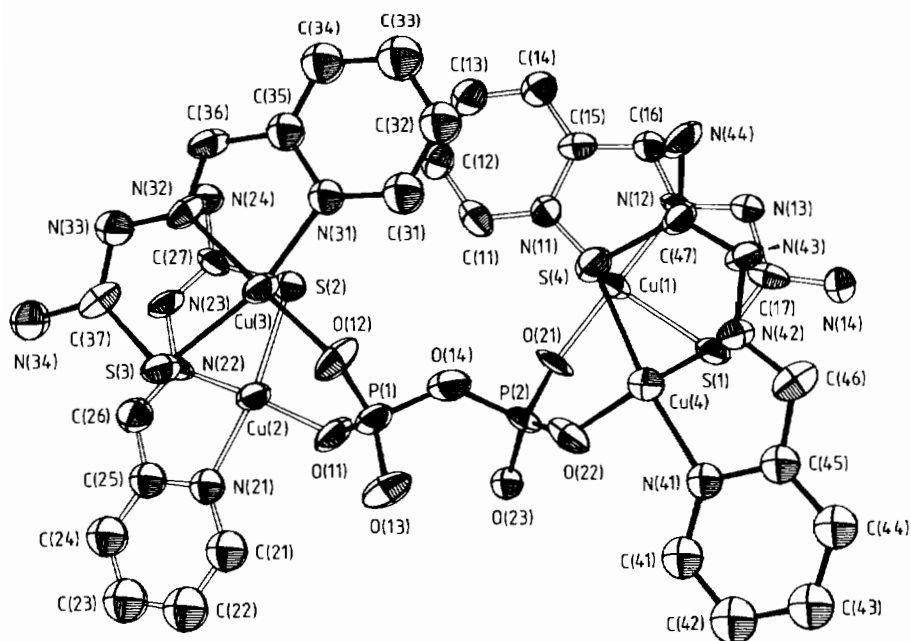


Fig. 1. The structure of the complex $[(\text{CuL})_4\text{P}_2\text{O}_7]$ showing the numbering system. Ellipsoids are drawn at the 50% probability level.

CuL^+ chromophore. The weaker d-d band observed near 650 nm is consistent with a square pyramidal geometry around the copper [17] similar to that found for the dimer $\{[\text{CuL}(\text{CH}_3\text{COO})_2]\}_2$ (λ_{max} 640 nm) [1]. However, it was the single crystal X-ray structure which revealed the interesting tetranuclear nature of the complex.

Crystal structure of $[(\text{CuL})_4\text{P}_2\text{O}_7] \cdot n\text{H}_2\text{O}$

The structure of the complex is shown in Fig. 1. It consists of a discrete tetranuclear species with a single pyrophosphate anion bridging four crystallographically distinct CuL^+ units. Selected bond distances and angles are given in Table 3.

The copper coordination sphere

The coordination spheres for the four Cu centres in the molecule are similar but not identical and may be described as distorted square pyramidal. Each copper is coordinated to the tridentate 2-formylpyridine thiosemicarbazone ligand, L, in the equatorial plane via the pyridine nitrogen, imine nitrogen and thioamide sulfur. The fourth equatorial position is occupied by a pyrophosphate oxygen. The coordination sphere is completed by a weak axial bond to a sulfur atom of an adjacent L ligand. There is no sixth contact of any significance.

The planes of 'best-fit' through the four equatorial donors around each of the four copper atoms show each copper to lie out of the plane towards the more weakly bound apical sulfur with a mean displacement of 0.126 Å. A significant distortion of the geometry

around Cu(4), towards a trigonal bipyramidal structure, is apparent when values of bond angles are compared with the equivalent angles for the other three copper atoms, Cu(1), Cu(2) and Cu(3). For instance the angles S(4)–Cu(4)–N(41) and N(41)–Cu(4)–S(1) at $160.2(2)^\circ$ and $98.0(3)^\circ$ (cf. the means of $164.4(9)$ and $90.7(1.2)^\circ$ found for the three other equivalent angles) are distorted towards 120° whereas O(22)–Cu(4)–S(1) at $92.8(3)^\circ$ (cf. the mean of $97.9(1.8)^\circ$ for the others) is nearer to 90° . The remaining angles around Cu(4) are not significantly different when compared with the averages of the equivalent bond angles for the atoms Cu(1), Cu(2) and Cu(3). The reasons for the distortion of the coordination sphere around Cu(4) away from square pyramidal towards a trigonal bipyramidal configuration are not obvious since the donor sets are equivalent and steric interactions with the tetranuclear species are expected to be equivalent. There are several significant differences in the copper–donor bond lengths (e.g. Cu(1)–N(12) and Cu(2)–N(22) have values of 1.920(7) and 1.973(8) Å, respectively) but no obvious pattern is observed in these.

The tetranuclear unit

Figure 1 shows each tetranuclear $[(\text{CuL})_4\text{P}_2\text{O}_7]$ molecule may be considered as a pair of dinuclear $(\text{CuL}^+)_2$ units linked by a $\text{P}_2\text{O}_7^{4-}$ anion. The dinuclear units are further linked by Cu–S axial bonds. These axial bonds range in length from 2.852(3) to 2.895(3) Å with a mean value of 2.881 Å and result in Cu...Cu separations of 3.288(2) and 3.231(2) Å for Cu(1)...Cu(4) and Cu(2)...Cu(3), respectively. Similar Cu–S axial

TABLE 1. Atomic coordinates ($\times 10^4$) for $[(\text{CuL})_4\text{P}_2\text{O}_7] \cdot n\text{H}_2\text{O}$ (standard deviations in parentheses)

Atom	x/a	y/b	z/c
Cu(1)	1942.7(0.4)	1117.6(0.5)	443.9(1.0)
Cu(2)	1286.5(0.4)	3557.2(0.5)	1467.2(1.1)
Cu(3)	1903.6(0.4)	3051.0(0.5)	3500.5(1.1)
Cu(4)	1210.1(0.5)	696.3(0.5)	1777.4(1.0)
S(1)	1479(1)	473(1)	-122(2)
S(2)	2045(1)	3340(1)	1547(2)
S(3)	1414(1)	3673(1)	3663(2)
S(4)	1945(1)	958(1)	2578(2)
P(1)	1067(1)	2510(1)	2036(2)
P(2)	1054(1)	1698(1)	641(2)
O(11)	990(2)	2943(3)	1358(6)
O(12)	1438(3)	2588(3)	3003(6)
O(13)	608(2)	2341(3)	2233(7)
O(14)	1287(2)	2100(3)	1449(6)
O(21)	1454(2)	1581(3)	115(6)
O(22)	921(3)	1280(3)	1256(7)
O(23)	628(2)	1905(3)	-83(7)
N(12)	2460(2)	680(3)	574(6)
N(13)	2402(3)	193(3)	430(6)
N(14)	1852(3)	-399(3)	65(7)
N(22)	1528(2)	4214(3)	1435(6)
N(23)	1984(3)	4317(3)	1580(6)
N(24)	2720(3)	3994(3)	1856(7)
N(32)	2402(2)	3490(3)	4123(6)
N(33)	2328(3)	3958(3)	4284(7)
N(34)	1775(3)	4555(3)	4153(7)
N(42)	1462(2)	71(3)	2255(6)
N(43)	1916(2)	-11(3)	2636(6)
N(44)	2642(3)	334(3)	3171(7)
C(16)	2881(3)	857(4)	842(8)
C(26)	1217(4)	4545(4)	1339(8)
C(36)	2830(3)	3318(4)	4331(8)
C(46)	1158(3)	-278(4)	2088(7)
C(11)	2468(4)	2063(4)	983(8)
C(12)	2865(4)	2316(4)	1228(9)
C(13)	3300(4)	2098(4)	1394(9)
C(14)	3316(4)	1612(4)	1275(9)
C(15)	2912(3)	1366(4)	1012(8)
N(11)	2482(3)	1590(3)	842(6)
C(17)	1949(3)	69(3)	167(7)
C(21)	242(4)	3731(5)	1212(9)
C(22)	-160(4)	4041(6)	1114(10)
C(23)	-96(4)	4501(6)	1099(11)
C(24)	351(5)	4705(5)	1165(10)
C(25)	727(3)	4387(4)	1231(8)
N(21)	672(2)	3915(3)	1266(6)
C(27)	2268(3)	3929(3)	1683(7)
C(31)	2451(4)	2122(4)	3498(8)
C(32)	2861(4)	1863(4)	3672(9)
C(33)	3283(4)	2088(4)	4043(10)
C(34)	3288(4)	2568(4)	4284(9)
C(35)	2865(3)	2825(3)	4120(8)
N(31)	2454(2)	2601(3)	3718(6)
C(37)	1880(3)	4079(4)	4049(8)
C(41)	161(3)	482(4)	1234(8)
C(42)	-242(3)	180(5)	1052(8)
C(43)	-161(4)	-306(4)	1209(8)
C(44)	311(3)	-483(4)	1517(7)
C(45)	671(3)	-140(4)	1691(7)
N(41)	600(2)	331(3)	1517(6)
C(47)	2171(3)	379(3)	2785(7)

interactions which link molecules into pairs or chains have been observed for several bis(thiosemicarbazone)copper(II) complexes [18–20] where the $\text{Cu} \cdots \text{Cu}$ separations are on average about 0.6 Å greater. Both pairs of copper atoms in the pyrophosphato complex also have a three-atom bridge from the pyrophosphato group, e.g. $\text{Cu}(1)-\text{O}(21)-\text{P}(2)-\text{O}(22)-\text{Cu}(4)$. A number of phosphato three-atom bridges between two copper atoms have been reported where the phosphato group is attached to a nucleotide [21, 22] but we are not aware of any other three-atom bridges involving pyrophosphates. The copper atoms in these nucleotide structures are separated by over 5 Å and are bridged by two phosphato groups. The angle between the two coordinated oxygens and the phosphorus in these structures of 113.2° is not significantly changed from the equivalent angles ($\text{O}(11)-\text{P}(1)-\text{O}(12)$ and $\text{O}(21)-\text{P}(2)-\text{O}(22)$) of 112.6(4) and 113.4(4)° in the complex $[(\text{CuL})_4\text{P}_2\text{O}_7]$.

In addition to these three-atom bridges, each copper in a 'dimer' has two, five-atom bridges to the coppers in the other 'dimer' with an average $\text{Cu} \cdots \text{Cu}$ separation of 7.31 Å (see Fig. 1). Overall, each copper is involved in a one-atom S bridge and a three-atom and two five-atom bridges via the coordinated pyrophosphato group. The magnetic behaviour of this complex cannot be explained using a simple dimer model (see below) and an interaction between 'dimers' has to be included to get a good fit to the data.

The pyrophosphate anion

The pyrophosphate anion in $[(\text{CuL})_4\text{P}_2\text{O}_7]$ appears to be unique in coordination chemistry. However, a number of salts (e.g. $\text{Na}_4\text{P}_2\text{O}_7$ [23] and $\alpha\text{-Mg}_2\text{P}_2\text{O}_7$ [24]) and binary compounds (e.g. $\alpha\text{-Cu}_2\text{P}_2\text{O}_7$ [25] and $\alpha\text{-Co}_2\text{P}_2\text{O}_7$ [26]) have been studied by X-ray diffraction

TABLE 2. Atomic coordinates ($\times 10^4$) and isotropic temperature factors for the water molecules in $[(\text{CuL})_4\text{P}_2\text{O}_7] \cdot n\text{H}_2\text{O}$ (standard deviations in parentheses)

Atom	x/a	y/b	z/c	U	Occupancy
O(101)	3511(3)	3381(4)	1955(7)	92(3)	1.0
O(102)	3980(4)	317(5)	1559(10)	129(4)	1.0
O(103)	3924(5)	3929(5)	5200(10)	146(5)	1.0
O(104)	3636(4)	802(4)	3746(9)	122(4)	1.0
O(105)	502(6)	1421(6)	2946(13)	74(4)	0.5
O(106)	4551(7)	1052(7)	1367(15)	91(5)	0.5
O(107)	4734(6)	3334(7)	4965(13)	78(5)	0.5
O(108)	288(5)	2599(5)	3866(11)	157(5)	1.0
O(109)	4446(6)	2043(6)	742(13)	74(4)	0.5
O(110)	4447(6)	1137(7)	3350(14)	83(5)	0.5
O(111)	4526(6)	2016(7)	4201(14)	84(5)	0.5
O(112)	4276(9)	2890(9)	3243(20)	137(9)	0.5
O(113)	4612(10)	3498(11)	1974(22)	144(10)	0.5

TABLE 3. Selected bond lengths^a (Å) and bond angles (°) with standard deviations in parentheses for the complex [(CuL)₄P₂O₇] \cdot *n*H₂O

Bond lengths			
Cu(1)–S(1)	2.279(3)	Cu(3)–S(3)	2.292(3)
Cu(1)–S(4)	2.888(3)	Cu(3)–S(2)	2.852(3)
Cu(1)–O(21)	1.904(7)	Cu(3)–O(12)	1.885(7)
Cu(1)–N(11)	2.030(7)	Cu(3)–N(31)	2.005(7)
Cu(1)–N(12)	1.920(7)	Cu(3)–N(32)	1.942(7)
Cu(2)–S(2)	2.266(3)	Cu(4)–S(4)	2.286(3)
Cu(2)–S(3)	2.895(3)	Cu(4)–S(1)	2.889(3)
Cu(2)–O(11)	1.916(7)	Cu(4)–O(22)	1.899(8)
Cu(2)–N(21)	2.014(8)	Cu(4)–N(41)	2.010(8)
Cu(2)–N(22)	1.973(8)	Cu(4)–N(42)	1.951(8)
S(1)–C(17)	1.747(9)	S(3)–C(37)	1.756(10)
S(2)–C(27)	1.768(9)	S(4)–C(47)	1.751(9)
N(12)–N(13)	1.383(11)	N(32)–N(33)	1.352(11)
N(12)–C(16)	1.294(11)	N(32)–C(36)	1.305(11)
N(13)–C(17)	1.331(11)	N(33)–C(37)	1.314(12)
N(14)–C(17)	1.341(13)	N(34)–C(37)	1.382(14)
N(22)–N(23)	1.328(10)	N(42)–N(43)	1.325(9)
N(22)–C(26)	1.281(13)	N(42)–C(46)	1.302(12)
N(23)–C(27)	1.354(12)	N(43)–C(47)	1.310(12)
N(24)–C(27)	1.296(12)	N(44)–C(47)	1.357(11)
C(15)–C(16)	1.442(15)	C(35)–C(36)	1.417(14)
C(25)–C(26)	1.468(14)	C(45)–C(46)	1.449(12)
Cu(1)...Cu(4)	3.288(2)	Cu(2)...C(3)	3.231(2)

Pyrophosphato bond lengths (Å)

P(1)–O(11)	1.502(8)	P(2)–O(21)	1.521(8)
P(1)–O(12)	1.504(7)	P(2)–O(22)	1.529(9)
P(1)–O(13)	1.493(8)	P(2)–O(23)	1.508(8)
P(1)–O(14)	1.603(8)	P(2)–O(14)	1.603(8)

Bond angles

S(1)–Cu(1)–S(4)	94.4(1)	S(3)–Cu(3)–S(2)	95.2(1)
S(1)–Cu(1)–O(21)	96.2(2)	S(3)–Cu(3)–O(12)	98.3(2)
S(1)–Cu(1)–N(11)	165.6(2)	S(3)–Cu(3)–N(31)	163.0(2)
S(1)–Cu(1)–N(12)	85.2(2)	S(3)–Cu(3)–N(32)	84.1(2)
S(4)–Cu(1)–O(21)	99.8(2)	S(2)–Cu(3)–O(12)	96.3(3)
S(4)–Cu(1)–N(11)	90.6(2)	S(2)–Cu(3)–N(31)	92.2(2)
S(4)–Cu(1)–N(12)	89.0(2)	S(2)–Cu(3)–N(32)	88.1(3)
O(21)–Cu(1)–N(11)	96.2(3)	O(12)–Cu(3)–N(31)	96.0(3)
O(21)–Cu(1)–N(12)	170.9(3)	O(12)–Cu(3)–N(32)	174.7(3)
N(11)–Cu(1)–N(12)	81.3(3)	N(31)–Cu(3)–N(32)	80.9(3)
S(2)–Cu(2)–S(3)	94.6(1)	S(4)–Cu(4)–S(1)	94.2(1)
S(2)–Cu(2)–O(11)	100.3(2)	S(4)–Cu(4)–O(22)	100.7(2)
S(2)–Cu(2)–N(21)	164.7(3)	S(4)–Cu(4)–N(41)	160.2(2)
S(2)–Cu(2)–N(22)	84.6(2)	S(4)–Cu(4)–N(42)	83.8(2)
S(3)–Cu(2)–O(11)	97.6(3)	S(1)–Cu(4)–O(22)	92.8(3)
S(3)–Cu(2)–N(21)	89.3(2)	S(1)–Cu(4)–N(41)	98.0(3)
S(3)–Cu(2)–N(22)	87.2(2)	S(1)–Cu(4)–N(42)	86.4(2)
O(11)–Cu(2)–N(21)	93.8(3)	O(22)–Cu(4)–N(41)	94.2(3)
O(11)–Cu(2)–N(22)	172.8(3)	O(22)–Cu(4)–N(42)	175.5(3)
N(21)–Cu(2)–N(22)	80.9(3)	N(41)–Cu(4)–N(42)	81.5(3)
Cu(1)–S(1)–C(17)	93.7(3)	Cu(3)–S(3)–C(37)	93.7(3)
Cu(2)–S(2)–C(27)	94.8(3)	Cu(4)–S(4)–C(47)	93.2(3)
Cu(1)–N(11)–C(11)	129.5(7)	Cu(3)–N(31)–C(31)	128.1(6)
Cu(1)–N(11)–C(15)	111.5(6)	Cu(3)–N(31)–C(35)	111.9(6)
Cu(1)–N(12)–N(13)	123.3(5)	Cu(3)–N(32)–N(33)	123.5(5)
Cu(1)–N(12)–C(16)	116.8(7)	Cu(3)–N(32)–C(36)	116.2(7)
N(12)–N(13)–C(17)	112.1(7)	N(32)–N(33)–C(37)	113.4(8)
N(11)–C(15)–C(16)	113.8(8)	N(31)–C(35)–C(36)	115.8(8)
N(12)–C(16)–C(15)	116.5(8)	N(32)–C(36)–C(35)	115.2(8)

(continued)

TABLE 3. (continued)

S(1)–C(17)–N(13)	124.6(7)	S(3)–C(37)–N(33)	124.2(8)
S(1)–C(17)–N(14)	118.4(6)	S(3)–C(37)–N(34)	118.7(7)
N(13)–C(17)–N(14)	116.9(8)	N(33)–C(37)–N(34)	117.1(8)
Cu(2)–N(21)–C(21)	127.2(8)	Cu(4)–N(41)–C(41)	130.4(8)
Cu(2)–N(21)–C(25)	112.9(6)	Cu(4)–N(41)–C(45)	111.9(6)
Cu(2)–N(22)–N(23)	123.2(6)	Cu(4)–N(42)–N(43)	123.4(6)
Cu(2)–N(22)–C(26)	115.6(7)	Cu(4)–N(42)–C(46)	115.3(6)
N(22)–N(23)–C(27)	114.0(8)	N(42)–N(43)–C(47)	113.4(7)
N(21)–C(25)–C(26)	114.6(9)	N(41)–C(45)–C(46)	115.0(8)
N(22)–C(26)–C(25)	116.0(10)	N(42)–C(46)–C(45)	115.7(9)
S(2)–C(27)–N(23)	122.5(7)	S(4)–C(47)–N(43)	124.7(7)
S(2)–C(27)–N(24)	119.0(7)	S(4)–C(47)–N(44)	117.2(7)
N(23)–C(27)–N(24)	118.4(8)	N(43)–C(47)–N(44)	118.0(8)

Pyrophosphato bond angles (°)

O(11)–P(1)–O(12)	112.6(4)	O(21)–P(2)–O(22)	113.4(4)
O(11)–P(1)–O(13)	110.2(4)	O(21)–P(2)–O(23)	112.8(5)
O(11)–P(1)–O(14)	107.8(5)	O(21)–P(2)–O(14)	102.3(4)
O(12)–P(1)–O(13)	113.1(5)	O(22)–P(2)–O(23)	111.7(4)
O(12)–P(1)–O(14)	103.7(4)	O(22)–P(2)–O(14)	107.2(5)
O(13)–P(1)–O(14)	109.1(4)	O(23)–P(2)–O(14)	108.8(4)
Cu(2)–O(11)–P(1)	132.5(4)	Cu(1)–O(21)–P(2)	130.3(5)
Cu(3)–O(12)–P(1)	136.4(5)	Cu(4)–O(22)–P(2)	135.4(5)
P(1)–O(14)–P(2)	132.9(4)		

^aC–H and N(X3)–H(X3) bond lengths fixed at 0.96 Å (X = 1–4).

techniques, hence a comparison of the bonding parameters can be made.

The P₂O₇⁴⁻ group comprises two slightly distorted PO₄ tetrahedra which share a common oxygen, O(14). Four of the six terminal oxygens are coordinated to four different copper atoms. The range of Cu–O bond lengths observed (1.885(7)–1.916(7) Å) is less than the values of 1.929, 1.935(13) and 1.95 Å found for the in-plane phosphato bonds in [Cu(5'-AMP)(bipy)-(H₂O)]₂(NO₃)₂·6H₂O (5'-AMP = adenosine 5'-monophosphate [22]), [Cu(5'-UMP)(dpa)(H₂O)]₂·5H₂O (5'-UMP = uridine 5'-monophosphate, dpa = 2,2'-dipyridylamine [21]) and for α-Cu₂P₂O₇ [24], respectively. In all of these instances the copper(II) atom is essentially five coordinate with the fifth axial coordination site occupied by an oxygen from water or pyrophosphate anion (average Cu–O_(axial) of 2.35 Å). This observed reduction in the in-plane Cu–O(phosphato) bond length in [(CuL)₄P₂O₇] \cdot *n*H₂O may therefore be a result of the weaker axial contact (average Cu–S_(axial) of 2.881(20) Å) accompanied by stronger in-plane coordination as well as the differences in the equatorial donor sets.

The two remaining terminal oxygens are not coordinated but are involved in hydrogen bonding to water molecules. As a result of this all six terminal P–O bonds (mean bond length 1.510(12) Å) show no significant bond length variation. The two bridging P–O bonds (mean distance 1.603(10) Å) are longer. The P(1)–O(14)–P(2) bridge angle is 132.9(4)°. A correlation has been observed between the bridge angle and the

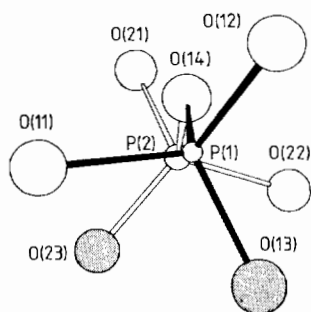


Fig. 2. The $\text{P}_2\text{O}_7^{4-}$ anion in the complex $[(\text{CuL})_4\text{P}_2\text{O}_7]$ showing the staggered arrangement.

difference between the experimentally observed bridging P–O and mean terminal P–O bond lengths, $\Delta d_{(\text{om})}$, and these agree well with the data reported for other pyrophosphates [27].

The $\text{P}_2\text{O}_7^{4-}$ anion can adopt either a staggered or an eclipsed conformation. In binary compounds with small cations the staggered orientation is preferred whereas with larger cations the eclipsed form tends to be favoured [28]. Figure 2 shows the pyrophosphate anion in $[(\text{CuL})_4\text{P}_2\text{O}_7] \cdot n\text{H}_2\text{O}$, with the plane containing P(1), O(14) and P(2) running vertically. From this diagram it can be seen that the $\text{P}_2\text{O}_7^{4-}$ moiety adopts a staggered configuration. For the ideal staggered arrangement the P(2)–O bonds should bisect the O–P(1)–O bond angles as the diagram is plotted, forming six angles of 60° . In $[(\text{CuL})_4\text{P}_2\text{O}_7]$, the mean OPPO torsion angle is only 42° . Factors such as the hydrogen-bonding network involving the pyrophosphate, and steric requirements for suitable bonding to copper will regulate this angle.

Hydrogen bonding

An extensive network of hydrogen bonds involving the pyrophosphate oxygens, the thioamide and amine nitrogens of L, and the water molecules exists in the structure of $[(\text{CuL})_4\text{P}_2\text{O}_7] \cdot n\text{H}_2\text{O}$ (Fig. 3) and must help to stabilize the crystal packing. The hydrogen bonding contact distances are listed in Table 4.

The pyrophosphate anion plays an integral role in the hydrogen bonding scheme and, except for the bridging and one coordinated oxygen (O(14) and O(12), respectively), all of the oxygen atoms are involved in hydrogen bonds to water molecules.

Figure 3 shows how the tetranuclear units stack one over the other. They are linked via shared hydrogen bonded water molecules and partial overlap of pyridine rings with approximately half of each ring involved in the overlap. The result is a stacking of the pyridine rings along the c axis with the distances of closest approach between the carbon atoms alternating between 3.194 and 3.297 Å. These approaches appear to be sufficiently close for some π overlap between rings to

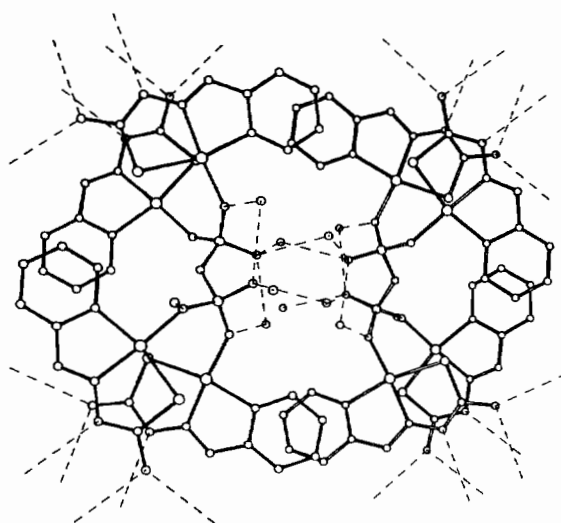


Fig. 3. Two $[(\text{CuL})_4\text{P}_2\text{O}_7]$ molecules with selected water molecules and hydrogen bonds. Hydrogen atoms have been omitted for clarity.

be possible [21, 22, 29]. Figure 3 also shows a number of hydrogen bonds from the thioamide nitrogens and the terminal amine nitrogens (N(X3) and N(X4) respectively where $X=1$ to 4) around the outside of the pairs of the tetranuclear molecules. One of the amine interactions is with a thioamide nitrogen on a symmetry related tetramer; this molecule then hydrogen-bonds back from its amine to the first thioamide nitrogen (average $\text{N} \cdots \text{N}$ contact of 2.991 Å). This results in pairs of tetramers being linked through such hydrogen-bonding contacts in a stepwise manner. A large number of the water molecules have been found to occupy spaces left by the molecular packing. These are involved in a hydrogen-bonding network amongst themselves and with the pyrophosphate oxygens and amine nitrogens and help in the stabilization of the structure. The overall effect, viewed down the c axis, as in Fig. 3, is to form a honeycomb type of packing arrangement, the walls of which are made up of the overlapping pairs of tetramers and the cavity containing the pyrophosphate moieties and water molecules.

Magnetic properties

The variable temperature magnetic susceptibility of the complex $[(\text{CuL})_4\text{P}_2\text{O}_7] \cdot n\text{H}_2\text{O}$ has been measured and, for comparison, that of the dimeric complex $[(\text{CuL}(\text{CH}_3\text{COO}))_2]$ is also given. As displayed for $[(\text{CuL}(\text{CH}_3\text{COO}))_2]$ in Fig. 4 the molecular susceptibilities show a rapid increase as the temperature approaches 0 K, with a maximum at approximately 6 K. Below 6 K the susceptibilities decrease, as is typical of weakly antiferromagnetically coupled copper(II) complexes. For the acetate complex the data were fitted very well by the Bleaney–Bowers expression [30] for

TABLE 4. Possible hydrogen bonding contacts for $[(\text{CuL})_4\text{P}_2\text{O}_7] \cdot n\text{H}_2\text{O}$

Atoms*	Distance (Å)	Symmetry site	Atoms*	Distance (Å)	Symmetry site
N(14)...N(33)	2.96	a	O(101)...O(112)	2.84	c
N(14)...O(103)	2.90	a	O(101)...O(113)	3.21	c
N(24)...N(43)	3.01	b	O(102)...O(106)	2.69	c
N(24)...O(101)	2.85	b	O(103)...O(105)	2.84	g
N(34)...N(13)	2.94	b	O(103)...O(107)	2.96	c
N(34)...O(102)	3.06	b	O(104)...O(110)	2.70	c
N(44)...N(23)	3.04	a	O(105)...O(105)	2.90	g
N(44)...O(104)	3.11	c	O(103)...O(107)	3.10	e
O(11)...O(109)	2.81	d	O(106)...O(110)	2.75	g
O(13)...O(108)	2.66	c	O(106)...O(110)	2.86	c
O(13)...O(108)	2.79	e	O(106)...O(109)	2.90	g
O(13)...O(105)	2.79	e	O(107)...O(112)	2.69	c
O(21)...O(101)	2.80	d	O(107)...O(108)	3.05	h
O(22)...O(105)	2.83	c	O(108)...O(111)	2.74	c
O(23)...O(107)	2.70	f	O(109)...O(111)	2.97	h
O(23)...O(113)	2.72	d	O(110)...O(111)	2.70	c
O(23)...O(109)	3.07	d	O(111)...O(112)	2.79	c
			O(112)...O(113)	2.73	c

*The first atom is at symmetry site c.

a: $(\frac{1}{2} - x, -\frac{1}{2} + y, \frac{1}{2} - z)$

c: (x, y, z)

e: $(\bar{x}, y, \frac{1}{2} - z)$

g: $(\frac{1}{2} - x, \frac{1}{2} - y, 1 - z)$

b: $(\frac{1}{2} - x, \frac{1}{2} + y, \frac{1}{2} - z)$

d: $(\frac{1}{2} - x, \frac{1}{2} - y, \bar{z})$

f: $(-\frac{1}{2} + x, \frac{1}{2} - y, -\frac{1}{2} + z)$

h: $(1 - x, y, \frac{1}{2} - z)$

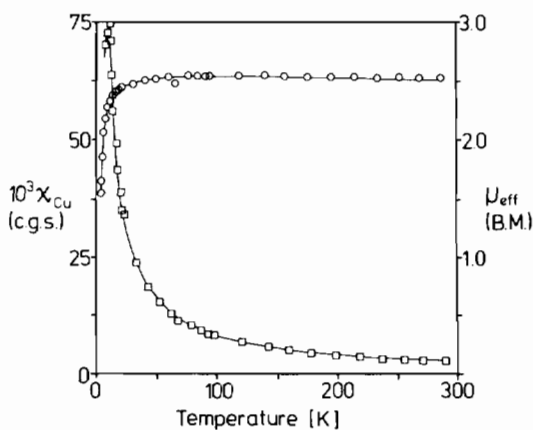


Fig. 4. Temperature dependence of the magnetic moment per two coppers (○) and molecular susceptibility per two coppers (□) for $[(\text{CuL}(\text{CH}_3\text{COO}))_2]$. The solid lines are those calculated using the parameters given in the text.

a spin coupled $S_1 = S_2 = \frac{1}{2}$ system with best-fit parameters of $g = 2.11$ and $2J = -6.2 \text{ cm}^{-1}$. The magnetic moment versus temperature plot depicted in Fig. 4 shows the moment to be nearly constant down to approximately 30 K. Below this temperature, the moment drops rapidly as spin-pairing of the two copper centres in the dimer occurs. The very low value of $2J$, the singlet-triplet splitting energy, presumably arises because of poor overlap of the magnetic orbitals. This is in accord with the crystal structure [1] which shows the dimer to have

acetato groups bridging the two copper atoms, stacking the two $\text{CuL}(\text{CH}_3\text{COO})$ moieties. The in-plane $\text{Cu}-\text{O}$ (acetato) bonding distance is $1.951(1) \text{ \AA}$ whereas the out of plane (apical) length is $2.427(2) \text{ \AA}$ with a $\text{Cu}-\text{O}-\text{Cu}'$ angle of $103.5(1)^\circ$. This long, off-axis, apical bond therefore may provide only weak overlap of the $d_{x^2-y^2}$ orbitals. In the structure of $[\text{Cu}_2\text{Cl}_2(\text{sap})_2] \cdot \text{dmf} \cdot \text{H}_2\text{O}$ ($\text{sapH} = \text{salicylaldehyde 2-amino-1-phenylethanol}$) the monoanionic, tridentate sap^- moiety coordinates in the plane with the fourth position occupied by a chloride ion (bond length of $2.261(2) \text{ \AA}$) [31]. The complex is a dimer, with the chloride ion forming a long bridge ($2.82(2) \text{ \AA}$) between the $\text{Cu}(\text{II})$ centres giving a distorted square pyramidal geometry. The magnetic susceptibilities, measured down to 5.1 K, showed a weak antiferromagnetic spin coupling which, on fitting to the Bleaney-Bowers equation, gave a value of $-7.1(4) \text{ cm}^{-1}$ similar to that found for $[(\text{CuL}(\text{CH}_3\text{COO}))_2]$.

The temperature dependence of the susceptibility and magnetic moment for the pyrophosphate complex, $[(\text{CuL})_4\text{P}_2\text{O}_7] \cdot n\text{H}_2\text{O}$, is similar to that observed for the acetate complex, although the χ_{Cu} values level off at very low temperatures rather than showing a definite maximum (Fig. 5). In view of the weakly associated 'pair of dimers' structure described above it was anticipated that a dimer model would be capable of fitting the magnetic data. However, this simple model tended to underestimate the size of the constant value of μ_{eff}

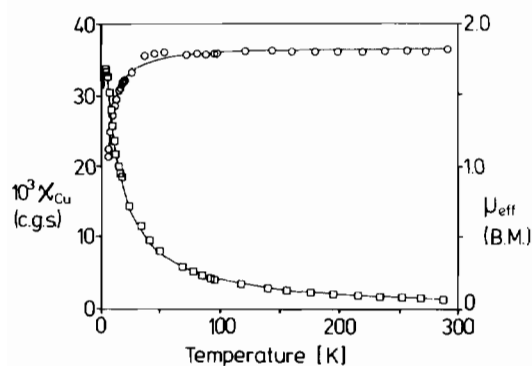


Fig. 5. Temperature dependence of the magnetic moment per copper (○) and the molecular susceptibility per copper (□) for $[(\text{CuL})_4\text{P}_2\text{O}_7] \cdot n\text{H}_2\text{O}$. The solid lines are those calculated using the parameters given in the text.

in the range 50–300 K although it reproduced the rapid decrease in μ_{eff} between 50 and 4.2 K. In such a fit the g value was also less than 2.0 (viz. 1.98) for $2J \approx -6 \text{ cm}^{-1}$. Comparison with related systems [32] suggested that nuances of this kind were generally indicative of interactions between dimers. Thus to allow for this effect the modified Bleaney–Bowers susceptibility expression containing a single J value and a $(T - \theta)$, rather than T , temperature term was employed [32]. As can be seen from Fig. 5 an excellent fit was obtained over the whole temperature range for parameter values $g = 2.14$ (from ESR $g_{\text{iso}} \approx 2.08$), $2J = -3.7 \text{ cm}^{-1}$ and $\theta = -3.6 \text{ K}$. Thus the intra- and intermolecular interactions are rather similar in size and sign. From structural considerations (*vide infra*) the $2J$ value is expected to correspond with the $\text{Cu}(1) \cdots \text{Cu}(4)$ and $\text{Cu}(2) \cdots \text{Cu}(3)$ pairs whereas the θ value results from interactions between these pairs. However the opposite could conceivably be the case. In other reported thiosemicarbazone systems, bridged by long Cu–S axial bonds, $2J$ values in the range -27 to -32 cm^{-1} [19, 33] have been obtained. However related sulfur-bridged copper dithiocarbamate complexes have $2J$ values closer to zero and in some cases positive [34]. The present compound has the added complication of the three-atom O–P–O bridge linking the copper–thiosemicarbazone planes and contributing to the net coupling between the $\text{Cu}(1) \cdots \text{Cu}(4)$ and $\text{Cu}(2) \cdots \text{Cu}(3)$ pairs. An exchange pathway of this type was found in a uridine 5′-monophosphate complex [35] for which a $2J$ value of -10.8 cm^{-1} was noted. Thus, the precise nature of the $\text{Cu}(1) \cdots \text{Cu}(4)$ and $\text{Cu}(2) \cdots \text{Cu}(3)$ coupling is not straightforward but is likely to be overall very weakly antiferromagnetic. The five-atom O–P–O–P–O pathways, i.e. between $\text{Cu}(1)$ and $\text{Cu}(3)$ or $\text{Cu}(2)$, while long in length, do connect ‘in-plane’ Cu orbitals and thus should yield antiferromagnetic J values of low magnitude. In general these

ideas are compatible with the fit obtained to the modified Bleaney–Bowers equation.

Conclusions

The isolation and characterization of the tetranuclear copper(II) complex, $[(\text{CuL})_4\text{P}_2\text{O}_7] \cdot n\text{H}_2\text{O}$, provides support for the suggestion that the phosphato groups of nucleic acids may bind to the (2-formylpyridine thiosemicarbazonato)copper(II) moiety *in vivo*. This will now prompt us to extend our studies to systems involving adenosine or uridine 5′-monophosphates in order to determine their binding modes to the CuL^+ ion. This study has further demonstrated the remarkable ability that the CuL^+ species has to bind a variety of anions [1, 8, 16], including more unusual ligands, such as the pyrophosphate group, to form crystalline products, with interesting structural and other physical features.

Supplementary material

Additional material for the structure, available from the Cambridge Crystallographic Centre, comprises H-atom parameters, thermal parameters and a complete listing of bond lengths and angles.

Acknowledgements

We thank the New Zealand University Grants Committee and the Australian Research Council for support. Mr C. Delfs is thanked for assistance with the fitting of the magnetic data.

References

- 1 A. G. Bingham, H. Bögge, A. Müller, E. W. Ainscough and A. M. Brodie, *J. Chem. Soc., Dalton Trans.*, (1987) 493.
- 2 C. F. Bell and C. R. Theocharis, *Acta Crystallogr., Sect. C*, **43** (1987) 26.
- 3 W. E. Antholine, B. Kalyanaraman and D. H. Petering, *Environ. Health Perspect.*, **64** (1985) 19, and refs. therein.
- 4 W. E. Levinson, *Antibiot. Chemother. (Washington, D.C.)*, **27** (1980) 288.
- 5 L. Thelander and P. Reichard, *Ann. Rev. Biochem.*, **48** (1979) 133.
- 6 W. Antholine and F. Taketa, *J. Inorg. Biochem.*, **20** (1984) 69.
- 7 W.E. Antholine, J. M. Knight and D. H. Petering, *Inorg. Chem.*, **16** (1977) 569.
- 8 E. W. Ainscough, A. M. Brodie, J. D. Ranford and J. M. Waters, *J. Chem. Soc., Dalton Trans.*, (1991) 1737.
- 9 B. J. Kennedy and K. S. Murray, *Inorg. Chem.*, **24** (1985) 1552; K. Bertocello, G. D. Fallon, J. H. Hodgkin and K.S. Murray, *Inorg. Chem.*, **27** (1988) 4750.

- 10 F. E. Anderson, C. J. Duca and J. V. Scudi, *J. Am. Chem. Soc.*, **73** (1951) 4967.
- 11 D. T. Cromer and J. B. Mann, *Acta Crystallogr., Sect. A*, **24** (1968) 321.
- 12 D. T. Cromer and D. Liberman, *J. Chem. Phys.*, **53** (1970) 1891.
- 13 R. A. Nyquist and R. O. Kagel, *Infrared Spectra of Inorganic Compounds*, Academic Press, New York, 1971.
- 14 W. J. Geary, *Coord. Chem. Rev.*, **7** (1971-72) 81.
- 15 B. J. Hathaway, in G. Wilkinson, R. D. Gillard and J. A. McCleverty (eds.), *Comprehensive Coordination Chemistry*, Vol. 5, Pergamon, Oxford, 1987, pp. 533-774.
- 16 E. W. Ainscough, E. N. Baker, A. M. Brodie, R. J. Cresswell, J. D. Ranford and J. M. Waters, *Inorg. Chim. Acta*, **172** (1990) 185.
- 17 L. T. Taylor and W. M. Coleman, *Inorg. Chim. Acta*, **63** (1982) 183.
- 18 M. R. Taylor, J. P. Glusker, E. J. Gabe and J. A. Minkin, *Bioinorg. Chem.*, **3** (1974) 189.
- 19 L. E. Warren and W. E. Hatfield, *Chem. Phys. Lett.*, **7** (1970) 371.
- 20 G. W. Bushell and A. Y. M. Tsang, *Can. J. Chem.*, **57** (1979) 603.
- 21 B. E. Fischer and R. Bau, *Inorg. Chem.*, **17** (1978) 27.
- 22 K. Aoki, *J. Am. Chem. Soc.*, **100** (1978) 7106, and refs. therein.
- 23 K. Y. Leung and C. Calvo, *Can. J. Chem.*, **50** (1972) 2520.
- 24 C. Calvo, *Acta Crystallogr.*, **23** (1967) 289.
- 25 B. E. Robertson and C. Calvo, *Acta Crystallogr.*, **22** (1967) 665.
- 26 N. Krishnamachari and C. Calvo, *Acta Crystallogr., Sect. B*, **28** (1972) 2883.
- 27 H. N. Ng and C. Calvo, *Can. J. Chem.*, **51** (1973) 2613.
- 28 G. M. Clark and R. Morley, *Chem. Soc. Rev.*, **5** (1976) 269.
- 29 L. Pauling, *The Nature of the Chemical Bond*, Cornell University Press, Ithaca, NY, 3rd edn., 1960.
- 30 B. Bleaney and K. D. Bowers, *Proc. R. Soc. London, Ser. A*, **214** (1952) 451.
- 31 F. Nepveu, F. Barmuth and L. Walz, *J. Chem. Soc., Dalton Trans.*, (1986) 1213.
- 32 T. M. Donlevy, L. G. Gahan, T. W. Hambley, G. R. Hanson, A. Markiewicz, K. S. Murray, I. L. Swann and S. R. Pickering, *Aust. J. Chem.*, **43** (1990) 1407.
- 33 W. E. Blumberg and J. Peisach, *J. Chem. Phys.*, **49** (1968) 1793.
- 34 A. J. van Duyneveldt, J. A. van Santen and R. Carlin, *Chem. Phys. Lett.*, **38** (1976) 585.
- 35 S. L. Lambert, T. R. Felthouse and D. N. Hendrickson, *Inorg. Chim. Acta*, **29** (1978) L223.